Supplemental material to the article

“Observation of Bosonic Resonances in $GdO_{1-x}F_xFeAs$ by Intrinsic Multiple Andreev Reflection Effect Spectroscopy”

In order to compare the shape of features in $dI(V)/dV$ spectrum caused by multiple Andreev reflections with possible boson emission with the features for the case of anisotropic gap, we use a simple model calculation. Fig. 1a shows theoretical curve

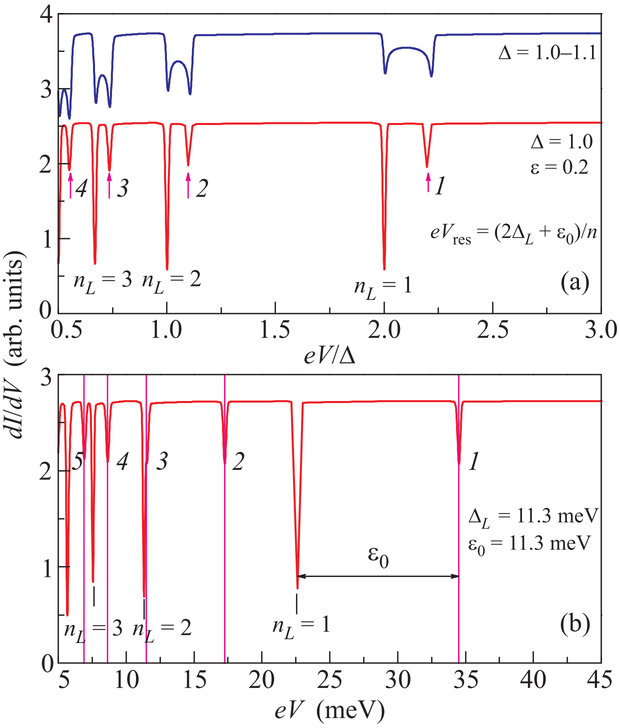

Figure 1: (a) – Fragments of $dI(V)/dV$ spectra demonstrating the position of expected Andreev subharmonic structures for the cases of (upper spectrum) anisotropic gap $\Delta = 1.0{-}1.1$, and (lower spectrum) isotropic gap $\Delta = 1$, and emission of a boson with energy $\varepsilon_0 = 0.2$. The gap subharmonics are marked with n_L labels, the satellite features caused by boson emission – with the corresponding n numbers and arrows. (b) – Similar calculation with the parameters resembling those determined in our studies of Gd-1111: $\Delta_L = 11.3\,\text{meV}$, $\varepsilon_0 = 11.2\,\text{meV}$. The data are simulated using the characteristic spectrum by Devereaux and Fulde [42] for the following parameters: clean isotropic superconductor, a ballistic SnS-contact ($l \gg 2a$), $T = 0$, $\Gamma = 0$, the exponential background of the $dI(V)/dV$ is suppressed

obtained by means of dynamic conductance integrating for the following cases: (i) a c-direction SnS-junction and in-plane anisotropic coupling of $cos(4\theta)$ type (the upper spectrum), and (ii) a boson emission keeping the isotropic superconducting gap $\Delta(\theta) = \Delta_0$ (the lower curve). The initial $dI(V)/dV$ spectrum for a clean isotropic superconductor and an “ideal” ballistic junction ($l \gg 2a$) at $T = 0$ are taken from the calculations in [42]. For the ballistic transport through SnS-junction, the in-plane Fermi velocities are several orders of magnitude larger than those out-of-plane at the applied bias voltages $V < 2\Delta/e$, and the carrier momenta are not mixed. Thus the c-direction transport is formally regarded as a combination of multiple parallel carrier channels, each with a certain coupling strength. The values of 2Δ and the weight coefficient corresponding to the channel contribution to the resulting conductance, are determined from the anisotropy type of the superconducting order parameter using the $1 + 0.5A[\cos(4\theta) - 1]$ expression, where the A coefficient is the percentage value of the gap anisotropy. For the upper curve in Fig. 1a, we take a representative value $A = 10\,\%$.

The lower curve in Fig. 1a qualitatively shows the gap subharmonics (the intensive dips at positions $eV_n = 2\Delta/n$,

$n = 1, 2, \ldots$, labeled with $n_L = 1, 2, \ldots$), and the boson-resonance caused features at $eV_{\text{res}}(n,k) = (2\Delta + k \cdot \varepsilon_0)/n$, where $k = 1, 2, \ldots$ is natural number of emitted bosons (labelled with the corresponding n numbers in accordance with formula (1) and arrows for $k = 1$). In order to reproduce the position of minima in the upper spectrum, for the lower $dI(V)/dV$ the gap was taken as unity, and the boson energy $\varepsilon_0 = 0.2\Delta$. In case of a small ε_0 as compared to Δ, obviously, the boson-caused features would be seen as satellite dips next to the SGS features. For the taken parameters, the first SGS dip is located at $eV_{n=1} = 2\Delta$, whereas the related satellite – at $eV_{\text{res1}} = 2.2\Delta$. Visually, each Andreev feature resembles a doublet, with the less pronounced dip at higher bias. The latter evidently follows from the probability of boson emission taken less than 50 %. Herewith, the boson-caused features comprise an additional subharmonic structure: the dynamic conductance between each gap subharmonic and boson- caused dip saturates enough to reach the background of $dI(V)/dV$. The latter strongly differs from the case of in-plane anisotropic gap (angle-dependent in a k-space) simulated by the upper curve in Fig. 1a . Given a weak 10 % gap anisotropy in a k-space (a four-fold symmetry widely discussed in literature with respect to Fe-based superconductors), one expects doublet features with the same positions of the dips but not so intensive and having another shape: both minima are asymmetric (the external sides of the doublet are abrupt whereas the inner ones are sloping) and connected by an arc, which couple does not reach the background of $dI(V)/dV$. Such arc structures were reproducibly observed by us in $dI(V)/dV$ spectra of Andreev contacts in $Ba_{1-x}K_xFe_2As_2$ and $BaFe_{2-x}Ni_xAs_2$ single crystals [30–32]. The obtained temperature dependences of both minima of the doublets look similar, therefore, we concluded the doublet as a single SGS feature caused by the gap anisotropy.

With the increasing gap anisotropy, the doublets become wider leading to the corresponding change in the positions of both dips; an impurity scattering Γ smears and widens the dips, anyhow, keeping their typical asymmetric lineshape and the arc structure. The latter is crucial to attribute experimental data to one of the above mentioned cases. The calculations and the $dI(V)/dV$ spectra for various gap symmetries are detailed in Fig. 4 in [21].

In the lower panel of Fig. 1, we simulated a dynamic conductance features taking the "realistic" values $\Delta_L = 11.3$ meV, $\varepsilon_0 = 11.2$ meV representative for Gd-1111 (see the text). In this case, the first bosonic resonance appears far beyond the $2\Delta_L$ singularity, the second feature $n_{\text{res}} = 2$ is located nearly midway between $2\Delta_L/e$ and Δ_L/e, whereas the third one $n_{\text{res}} = 3$ gets exactly the position of the second subharmonic Δ_L/e. Note that at any temperatures up to T_C, the position of Andreev features directly determines the energy parameters of superconductor [23, 26].

In order to create SnS-junctions and Andreev SnSn-. . . -S arrays using the "break-junction" technique, a plate-like sample was mounted onto a springy sample holder and cooled down to $T = 4.2$ K. Then, under a gentle mechanical curving of the holder the crystal was cracked with a formation of two cryogenic surfaces separated with a weak link. During the experiment, the crack is kept in the bulk of the sample, thus making clean cryogenic clefts and preventing their degradation [21]. In Gd-1111, the weak link often acts as a thin normal metal [5–8], thus demonstrating $I(V)$ and $dI(V)/dV$ curves similar to those for a clean classical SnS-contact [23–26].

In layered compounds, steps and terraces on cryogenic clefts may realize SnSn-. . . -S arrays typical for the break-junction studies [21]. Layered crystal grains with the ab crystallographic planes oriented parallel to the crack plane cleaved when making a crack, demonstrate steps and terraces [7,21]. The cryogenic clefts slide apart each other, touching through the terrace. Under a gentle mechanical readjustment, the touching point hops between the neighbour terraces forming Andreev arrays with various area and number of junctions, likewise in the single crystal. Since the array is a sequence of m identical SnS junctions, intrinsic multiple Andreev reflections effect (IMARE) occurs there, causing scaling of positions of any features caused by the bulk with natural number m. In particular, the SGS would be observed at $V_n = 2\Delta_{L,S} \times m/en$. According to our estimates, the average diameter of each weak link is about $10 - 30$ nm, therefore, the IMARE probes the superconducting energy parameters locally. The actual number of junctions m in the array could be determined when normalize the $dI(V)/dV$ to that of single junction [8, 21]. Herewith, probing such arrays as a bulk natural structures is favourable for many reasons [21]. Summarizing the above mentioned, the described technique is a powerful probe of energy parameters of superconductor. The high quality of break junctions gives an opportunity to resolve a clear fine structure in dynamic conductance spectra, and therefore to study electron-boson interaction. The IMARE spectroscopy realized by the "break-junction" technique is therefore a direct local probe providing a highly accurate bulk values of characteristic energy parameters [21].

The numbering of the references is made in accordance with the full text.